Published in : Macromolecules (2019), vol.52x, n°52, pp. 444–456
DOI: 10.1021/acs.macromol.8b02188
Status : Postprint (Author's version)

PHOTO-CROSS-LINKABLE COUMARIN-BASED POLY(ε-CAPROLACTONE) FOR LIGHT-CONTROLLED DESIGN AND RECONFIGURATION OF SHAPE-MEMORY POLYMER NETWORKS

Thomas Defize,[†] Jean-Michel Thomassin,[†] Heidi Ottevaere,[‡] Cedric Malherbe,[§] Gauthier Eppe,[§] Rachid Jellali,[†] Michael Alexandre,[†] Christine Jerôme,[*,†] and Raphael Rivä[†]

[†]*Centre for Education and Research on Macromolecules (CERM), CESAM Research Unit, University of Liege (ULiege), Allée du 6 août 13, Building B6a, 4000 Liege, Belgium*
[‡]*Brussels Photonics (B-PHOT), Department of Applied Physics and Photonics (TONA), Vrije Universiteit Brussel (VUB), Pleinlaan 2, 1050 Brussels, Belgium*
[§]*Laboratory of Inorganic Analytical Chemistry, MolSys Research Unit, University of Liege (ULiege), Building B6c, 4000 Liège, Belgium*

ABSTRACT

Photochemically cross-linked shape-memory polymer (SMP) materials have been achieved by functionalizing chain-ends of star-shaped poly(ε-caprolactone) (PCL) with 7-hydroxypropoxy-4-methylcoumarin followed by photodimerization of these end-groups. The kinetics of the network formation in function of the photosensitizer concentration has been studied by swelling experiments and rheology. Thanks to the design of a dedicated homemade mold, highly reproducible irradiation conditions have been achieved allowing to study the network formation and properties, especially the shapememory properties, in relation to the coumarin dimerization degree as determined by Raman spectroscopy. In optimized conditions, PCL-based SMP materials exhibiting high fixity and recovery have been achieved in remarkably short irradiation time, typically 5 min. In addition, the precise control of the network cross-link density with the irradiation time, so as the high stability of the formed networks toward temperature variations was also demonstrated allowing the fine-tuning of the network properties by the irradiation process. Finally, the reversible character of the coumarin dimerization under light irradiation of appropriate wavelength has been quantified by Raman spectroscopy. The dimer photocleavage allows the photoreconfiguration of the networks offering the ability to modify the "permanent" shape of the SMP material, while preserving the excellent shape-memory properties.

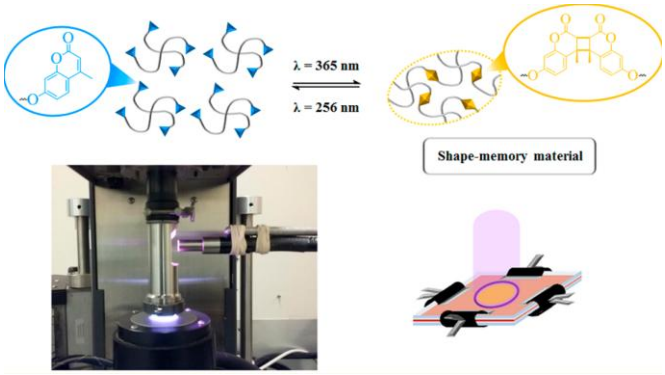

Published in : Macromolecules (2019), vol.52x, n°52, pp. 444–456
DOI: 10.1021/acs.macromol.8b02188
Status : Postprint (Author's version)

INTRODUCTION

Shape-memory polymers (SMPs) are a class of materials presenting the remarkable property to recover a macroscopic "permanent" shape from a stable "temporary" shape, induced under specific conditions of stress and temperature, by the application of an appropriate stimulus.[1]−[3] SMP materials are already successfully applied as thermal sensors and actuators,[4]−[7] as smart textiles,[8] or as smart medical devices allowing minimally invasive surgery.[2],[9] Typically, the permanent shape is determined during processing by chemical (covalent bonds) or physical (intermolecular interactions) cross-linking of the polymer matrix. On the other hand, the temporary shape is obtained by the heating of the SMP material above a transition temperature, e.g., glass or melting transition, followed by the application of a mechanical stress leading to the deformation of the material. The temporary shape is then fixed by cooling below the transition temperature under stress, leading to the reformation of glassy domains or crystallites (switching domains). The heating of the SMP material above the transition temperature in stress-free conditions induces the collapse of the switching segments, leading to the relaxation of the SMP material to the permanent shape as a result of entropy elasticity. When irreversible reactions are used to cross-link the polymer matrix, the reprocessing of the permanent shape is impossible without breaking some bonds in the main chain, limiting or even preventing the recycling of the SMP materials. Thereby, the use of reversible reactions, allowing the formation/cleavage of the network, raised tremendous interest in the past years for the development of reprocessable SMP materials.[10],[11] When such reaction is only partially reversible so that the network does not cross back the gel point, the sample gains plasticity even if it is not flowing. In that case, the recycling is no more achieved, but the shape reconfiguration of the material is made possible by the so-called solid-state plasticity, which is especially useful when complex origami structures deploying upon shape-memory thermal transition are targeted.

In this context, some of us recently reported on the synthesis of a well-defined reversibly cross-linked PCL-based SMP material by the Diels−Alder (DA) reaction between furan and maleimide, well-known to create thermoreversible bonds. After processing, this recyclable SMP material was characterized by excellent fixity and recovery before and after recycling experiments.[12],[13] In this system, strong reversibility of the DA adduct allows to cross back and forth the gel point, making recycling of the material very efficient. In contrast, the rapid flowing of the sample at high temperature makes the solid-state plasticity reconfiguration of such material quite tricky. In addition, drawbacks of this system are the long curing time imposed by the kinetic of the DA adduct formation between furan and maleimide and the creep occurring upon repeating shape-memory cycles due to the thermoinstability of the DA adducts.[14]

To build covalent networks, photoinduced cross-linking is an interesting alternative because the light-induced process is economical, easy, rapid, and nondestructive and can be localized as well as remotely activated.[15],[16] Therefore, lightinduced cross-linking of polymers containing photoreactive functional groups is also extensively reported.[17] In addition, the cross-linking can also be photoreversible when the photodimerization of cinnamoyl, anthracene, or coumarin groups is selected for the cross-linking process.

Published in : Macromolecules (2019), vol.52x, n°52, pp. 444–456
DOI: 10.1021/acs.macromol.8b02188
Status : Postprint (Author's version)

In the 1990s, Chen and co-workers applied the photodimerization of coumarin derivatives to cross-link poly(vinyl acetate),[18] polyacrylates,[19] and polyamides,[20] allowing the formation/cleavage of the polymer network under UV irradiation at 350 or 254 nm, respectively. They also demonstrated that the dimerization of 4-methylcoumarin was 3 times faster at 350 nm compared to that of coumarin[18] while the addition of a photosensitizer, such as benzophenone, increased the dimerization rate without affecting the photocleavage rate.[21] More recently, Rivero et al. reported on the photo-cross-linking of coumarin-PCL-based polyurethanes as healing coatings.[22],[23]

In the field of SMP materials, cinnamates,[24]−[26] cinnamamide,[25],[27] cinnamylidene acetate,[24] and anthracene[28],[29] photodimerization was judiciously applied to fix the temporary shape at a precise wavelength, typically >260 nm, allowing the formation of switching domains by dimerization photoreactions. The UV irradiation of the SMP material at a lower wavelength (<260 nm) in stress-free conditions leads to the cleavage of the dimers and thus to the relaxation of the material to its permanent shape.

Photodimerization reactions were also successfully applied by other groups for the preparation of thermally induced SMPs.[26],[30],[31] When PCL-based SMP materials are considered, Nagata et al. reported on the synthesis of coumarin bearing copolyesters by polycondensation reaction between PCL-diol and a diacyl chloride bearing a coumarin pendant group, allowing the formation/cleavage of the network by a photoreversible [2 + 2] cycloaddition reaction, characterized by good shape-memory properties.[32],[33]

This paper aims at introducing these thermostable but photoreversible coumarin dimers into semicrystalline 4-arm star-shaped PCL networks in place of the previously reported[12]−[14] thermoreversible furan−maleimide Diels−Alder adducts with the goal to (i) preserve the excellent fixity and recovery of the 4-arm star-shaped PCL network while preventing the creep thanks to thermal stability of the coumarin dimer and (ii) impart a light control rather than a thermal control of the network cross-linking (Scheme 1). This novel material is expected to exhibit thermally induced shapememory properties combined with possible light control of the network cross-linking density, i.e., mechanical properties, photoinduced recycling, and/or photocontrolled permanent shape reconfiguration.

Scheme 1. Coumarin-Based Photo-Cross-Linkable Star-Shaped PCL for Light-Controlled Design of Networks (at 365 nm) and Shape Reconfiguration (at 256 nm)

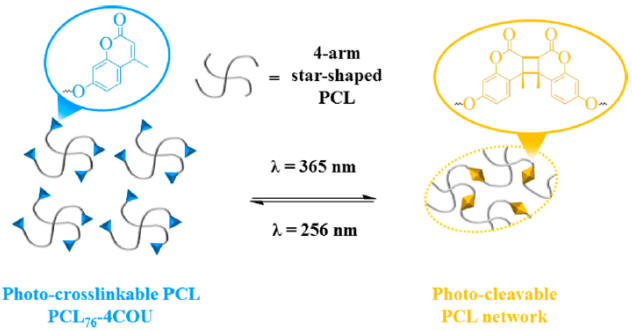

For this purpose, the well-defined 4-arm star-shaped PCL is functionalized at each chain-end by 4methylcoumarin moieties, then processed into films by compression molding, and cross-linked by

Published in : Macromolecules (2019), vol.52x, n°52, pp. 444–456
DOI: 10.1021/acs.macromol.8b02188
Status : Postprint (Author's version)

coumarin dimerization under irradiation at 365 nm (Scheme 1). The crosslinking density of these PCL networks is studied as a function of the UV curing time and light wavelength. The kinetics of the network formation as a function of the photosensitizer concentration is followed by swelling experiments and rheology, and the dimerization degree by Raman spectroscopy leading to very short UV curing time (5 min) in optimized conditions. Thermally induced shape-memory properties of the cross-linked PCL, i.e. fixity and recovery are studied using a dynamical mechanical analyzer (DMA). The reversibility of the coumarin dimerization is carefully studied by Raman spectroscopy and rheology and advantageously used for the reconfiguration of the permanent shape of this new SMP material by solid-state plasticity.

EXPERIMENTAL SECTION

Materials. Toluene (Chem-lab), tetrahydrofuran (THF, Chemlab), methanol (Chem-lab), dichloromethane (CH_2Cl_2, Chem-lab), diethyl ether (Chem-lab), *N,N*-dimethylformamide (DMF, Aldrich), succinic anhydride (Aldrich), triethylamine (NEt_3, Aldrich), dicyclohexylcarbodiimide (DCC, Aldrich), *N,N*-dimethyl-4-aminopyridine (DMAP, Aldrich), 7-hydroxy-4-methylcoumarin (Aldrich), ethanol (VWR Chemicals), 3-bromo-1-propanol (Aldrich), potassium carbonate (Aldrich), and benzophenone (Aldrich) were used as received. CAPA 4801 (4-arm star-shaped PCL (PCL_{76}-4OH), M_n = 8800 g/mol, $Đ$ = 1.2) was kindly offered by Perstorp. Toluene was dried on molecular sieves and kept under an inert atmosphere.

Synthesis of 7-Hydroxypropyl-4-methylcoumarin. 17 g (96 mmol) of 7-hydroxy-4-methylcoumarin was dissolved into 600 mL of anhydrous DMF in a previously dried glass reactor. 66 g (480 mmol) of potassium carbonate and 20 g (144 mmol) of 3-bromo-1-propanol were added to the solution, and the mixture was stirred at 70 °C overnight. The solution was then cooled to room temperature before being filtered to remove the excess of potassium carbonate. After elimination of DMF under vacuum, the solid was collected with 200 mL of ethanol, and the solution was filtered again to remove the residual traces of potassium carbonate. Ethanol was removed under vacuum, and the solid was redissolved in a minimal amount of methanol and recrystallized two times in toluene upon cooling. A light-yellow solid was recovered by filtration and vacuum-dried (yield: 48%). Melting point = 91−93 °C. ^{1}H NMR (400 MHz, methanol-d_4): δ = 2.05 (2H, q, CH_2−CH_2−CH_2−), 2.46 (3H, s, CH_3), 3.79 (2H, t, CH_2−OH), 4.2 (2H, t, CH_2−O), 6.17 (1H, s, =CH−CO), 6.86−7(2H, m, H aromatic), 7.68 (1H, d, H aromatic) (Figure S1). ^{13}C NMR (100 MHz, methanol-d_4): δ = 18.94 (CH_3), 33.39 (CH_2−CH_2−CH_2), 59.6 (CH_2−OH), 66.77 (CH_2−O), 102.47 (aromatic C, O−C−CH═C), 112.28 (C═CH−CO), 114.17 (aromatic C, O−C═CH−CH=), 114.91 (quaternary aromatic C, CHC−C(CH_3)), 127.45 (aromatic C, O−C═CH−CH═), 155.9 (quaternary C, C−CH_3), 156.59 (quaternary aromatic C, CH═C−O−CO), 163.77 (quaternary aromatic C, CH_2−O−C), 164.08 (C═O). ATR IR ν (cm^{-1}): 3411 (O−H), 1698 (C═O), 1604 (C═C).

Synthesis of 4-Arm Star-Shaped Carboxylic Acid EndCapped PCL (PCL_{76}-4COOH). 20 g (10 mmol of hydroxyl function) of PCL_{76}-4OH was transferred into a previously dried glass reactor. After three azeotropic distillations with anhydrous toluene, 100 mL of anhydrous DMF was added to the reactor through a rubber septum with a stainless steel capillary. After complete solubilization, 1.1 g (11 mmol) of succinic anhydride and 1.55 mL (11 mmol) of NEt_3 were sequentially added to the DMF solution. The

Published in : Macromolecules (2019), vol.52x, n°52, pp. 444–456
DOI: 10.1021/acs.macromol.8b02188
Status : Postprint (Author's version)

solution was then stirred at 45 °C overnight. PCL_{76}-4COOH was recovered by precipitation in diethyl ether, filtered, and dried under vacuum. ^{1}H NMR (400 MHz, $CDCl_3$): δ = 1.37−1.64 (456H, m, $C\underline{H}_2-C\underline{H}_2-C\underline{H}_2$), 2.30 (152H, t, $C\underline{H}_2-C(O)$), 2.61 (16H, s, $C(O)-C\underline{H}_2-C\underline{H}_2-$ C(O)), 4.05 (152H, t, $C\underline{H}_2-O-C(O)$). M_n(^{1}H NMR) = 9200 g/ mol, $Đ$(SEC) = 1.15.

Synthesis of 4-Arm Star-Shaped Coumarin End-Capped PCL (PCL_{76}-4COU). 17.8 g (7.8 mmol of carboxylic acid functions) of PCL_{76}-4COOH was dissolved into a glass reactor containing 100 mL of anhydrous dichloromethane. 2.5 g (10.6 mmol) of 7-hydroxypropyl-4-methylcoumarin, 2.29 g (10.6 mmol) of DCC, and 0.27 g (2.12 mmol) of DMAP were then added, and the solution was stirred at 25 °C overnight. The solution was filtered to remove DCU (dicyclohexylurea), and PCL_{76}-4COU was recovered by precipitation in cold diethyl ether, filtered, and dried under vacuum. ^{1}H NMR (400 MHz, $CDCl_3$): δ = 1.37−1.64 (456H, m, $C\underline{H}_2-C\underline{H}_2-C\underline{H}_2$), 2.15 (7.6H, quintuplet, $O-CH_2-C\underline{H}_2-CH_2-O$), 2.20−2.42 (152H, t, $C\underline{H}_2-C(O)$ PCL + 11,4 H, s, $C\underline{H}_3$), 2.62 (15.2H, s, $C(O)-C\underline{H}_2-$ $C\underline{H}_2-C(O)$ + 0.8H, s, $C(O)-C\underline{H}_2-C\underline{H}_2-C(O)OH$), 4.05 (152H, t, $C\underline{H}_2-OC(O)$ PCL+ $Ph-O-CH_2-CH_2-C\underline{H}_2-O-C(O)$), 4.30 (7.6H, t, $C\underline{H}_2-O-Ph$), 6.13 (3.8H, s, $C_H{=}C$), 6.78−6.88 (7.6H, d, H aromatic) 7.48 (3.8H, d, H aromatic).

Photo-Cross-Linking of Coumarin End-Capped 4-Arm StarShaped PCL. *Without Photosensitizer*. 0.35 g of PCL_{76}-4COU was placed in a circular template of 25 mm diameter and 0.5 mm thick cut in a metal plate and processed by compression molding at 80 °C. A homemade mold allowing light irradiation at 60 °C has been designed to prevent the formation of an irregular surface during UV irradiation and ensure reproducibility. The template containing the PCL sample was sandwiched between two films made of cross-linked polydimethylsiloxane (PDMS) (the synthesis of the PDMS membranes is reported elsewhere[34]), preventing the adhesion of cross-linked PCL to the quartz plates used to provide rigidity, which are both transparent to UV irradiation. The system was then fixed with four clamps to maintain together the different parts and placed under UV irradiation at 365 nm in a ventilated oven at 60 °C. The photocuring at 365 nm was performed with an OmniCure Series 2000 (200 W, 365 nm) for 120 and 360 min for PCL_{76}-4COU-$Bzph_0$120min and PCL_{76}-4COU-$Bzph_0$-360min, respectively.

With Photosensitizer. Typically, 1 g (0.376 mmol of coumarin) ofPCL_{76}-4COU was mixed with 17 mg (0.094 mmol) (PCL_{76}-4COU$Bzph_{25}$) or 34 mg (0.188 mmol) (PCL_{76}-4COU-$Bzph_{50}$) of benzophenone before being dissolved in 5 mL of toluene. After evaporation of toluene under vacuum, the blends were then processed as described above for the system without photosensitizer except that the photocuring times at 365 nm were equal to 60, 30, and 5 min for

PCL_{76}-4COU-$Bzph_{25}$-60min, PCL_{76}-4COU-$Bzph_{50}$-30min, and PCL_{76}-4COU-$Bzph_{50}$-5min, respectively.

Photocleavage of the Coumarin Dimer in the Network. The cleavage of the coumarin dimers in the PCL matrix was performed with a 256 nm laser beam. A frequency-doubled Nd:YAG pump laser (Spectra-Physics Millennia Prime 10sJSPG) pumps a tunable titanium-sapphire laser (Spectra-Physics Tsunami laser) of which the fundamental laser light is directed toward a harmonic-generating unit, comprising a second- and third-harmonic generating crystal, to generate UV excitation wavelengths. To obtain 256 nm laser light, the third-harmonic generating crystal enabling wavelengths between 240 and 275 nm was selected, with a maximal output power between 60 and 200 mW. After the selection of the 256 nm laser line, the laser light (power of 70 mW) was directed toward the sample by the use of an additional lens (Newport KPX181) to enlarge the laser beam to a diameter of 3 cm, slightly greater than the diameter of the sample (2.5 cm).

Published in : Macromolecules (2019), vol.52x, n°52, pp. 444–456
DOI: 10.1021/acs.macromol.8b02188
Status : Postprint (Author's version)

Swelling Experiments. Flat sheets of cross-linked PCL samples (around 0.1 g) collected after UV curing were placed separately into 30 mL chloroform, a good solvent for PCL, for 24 h at room temperature. Then the swollen sheet (gel) is carefully collected and weighed. w_i is the initial mass of the sheet, and w_s is the mass of the gel (swollen network weight). Finally, the gel was dried under vacuum until reaching constant weight, w_d (dried network weight). The swelling ratio (SR) and the gel content (GC) (= insoluble fraction, i.e., network fraction) were calculated based on these weight measurements according to eqs 1 and 2, respectively.

$$\mathrm{SR} = \frac{w_s - w_d}{w_d} \times 100 \quad (1)$$

$$\mathrm{GC}\ (\%) = \frac{w_d}{w_i} \times 100 \quad (2)$$

Characterization Techniques. SEC was performed in THF at 45 °C at a flow rate of 1 mL/min with a Viscotek 305 TDA liquid chromatograph equipped with two PSS SDV linear *M* columns calibrated with polystyrene standards. ^{1}H NMR spectra were recorded in $CDCl_3$ or methanol-d_4 at 400 MHz in the FT mode with a Bruker Avance 400 apparatus equilibrated at 25 °C.

Raman spectra were recorded at room temperature using a HoribaJobin-Yvon Labram 300 confocal spectrometer equipped with an Olympus BX40 microscope. The excitation wavelength was 785 nm, and the laser was focused on a rectangular-shaped solid sample with an Olympus ×100 objective. The laser power at the sample level was of the order of 15 mW. Every spectrum was accumulated twice for about 10 s or more depending on the sample signal. The detector is an Andor iDus BR-DD 401 CCD. All spectra were scaled up and, if necessary, baseline corrected with homemade software. The Raman spectra of the samples before and after UV irradiation were recorded with a laser at 785 nm at room temperature from 1000 to 1800 cm^{-1}. It is noteworthy that all the Raman analyses were performed on both sides of the samples and that both spectra were perfectly superimposed on each other. Besides the Raman bands of PCL, the analysis of PCL_{76}-4COU precursor revealed characteristic bands of coumarin groups at 1617, 1562, 1514, and 1393 cm^{-1} (stretching modes of C═C), 1372 cm^{-1} (symmetric bending vibration of methyl group), 1346 cm^{-1} (in-plane CH bending vibration ring), 1206 cm^{-1} (symmetric C(O)−O−C stretching vibrations mode), and 1157 cm^{-1} (in-plane rocking vibration mode of methyl group). These bands decrease upon dimerization of coumarin. The Raman band at 1617 cm^{-1} is frequently selected to follow the conversion of the coumarin in the corresponding dimer as it is the more intense band related to the stretching vibration mode of C═C of the pyrone ring.[35] However, this band overlaps with another band at 1624 cm^{-1}, corresponding to the stretching mode of C═C of the benzene ring of coumarin and does not allow a precise determination of the dimerization yield. The use of the band at 1562 cm^{-1}, corresponding to the stretching mode of C═C of the pyrone ring, is more relevant as no contribution of other bands is observed. First, Raman spectra were normalized using the methylene Raman band of the PCL at 1442 cm^{-1} as reference since it remains constant before and after UV irradiation. The conversion of the coumarin as a function of the UV irradiation time at 365 nm was then calculated using the ratio between the intensity of the band at 1562 cm^{-1} before (t_0) and after (t) UV irradiation, according to eq 3.

Published in : Macromolecules (2019), vol.52x, n°52, pp. 444–456
DOI: 10.1021/acs.macromol.8b02188
Status : Postprint (Author's version)

$$\text{coumarin conversion } (\%) = \left(1 - \frac{I_{1562\ \text{cm}^{-1}}(t)}{I_{1562\ \text{cm}^{-1}}(t_0)}\right) \times 100 \qquad (3)$$

Rheological measurements were performed using an ARES-G2k rheometer from TA Instruments equipped with an ARES-G2 curing accessory, made of a light guide, a quartz plate, and a reflecting mirror assembly allowing the transfer of the UV irradiation from the UV-light source to the sample (Figure S3). Typically, 0.25 g of a disk was placed at 60 °C between a plate−plate geometry (diameter 20 mm, thickness 0.5 mm), and both the elastic and viscous moduli were recorded through time at a frequency of 1 Hz and a strain of 1% under UV irradiation at 365 nm. The frequency sweep was performed at 60 °C from 0.025 to 15.9 Hz at a strain of 1% (Figure S4).

Differential scanning calorimetry (DSC) was performed using a DSC Q500 (TA Instruments) calibrated with indium by the following "heating/cooling/heating" procedure: heating at 3 °C/min to 100 °C, cooling at 3 °C/min to −80 °C, and heating at 3 °C/min to 100 °C. The T_m and melting enthalpy (ΔH_m) were recorded during the second heating ramp.

Shape-memory properties were measured with a DMA Q800 (TA Instruments) using the tensile film clamp in controlled force mode. The sample (typically 5 mm × 5 mm × 0.5 mm) was first equilibrated at 65 °C for 5 min and then experienced a tensile stress ramp (0.06 MPa/min) until 0.6 MPa, except for PCL_{76}-4COU-$Bzph_{50}$-5min which experienced a stress of 0.3 MPa (0.06 MPa/min). Subsequently, the sample was cooled down, under stress at 3 °C/ min to 0 °C (for PCL_{76}-4COU-$Bzph_0$-120min, PCL_{76}-4COU-$Bzph_0$360min, and PCL_{76}-4COU-$Bzph_{50}$-5min) or to −30 °C (for PCL_{76}4COU-$Bzph_{25}$-60min and PCL_{76}-4COU-$Bzph_{50}$-30min) and maintained at that temperature for 5 min. The stress is finally released and the sample is reheated, stress-free at 3 °C/min to 65 °C. The cycle is repeated four times.

RESULTS AND DISCUSSION

PCL Precursors Synthesis. As reported in previous papers,[12]−[14] end-group functionalization of 4-arm star-shaped PCL of 8800 g/mol (PCL_{76}-4OH) by furan or maleimide provides materials able to be efficiently cross-linked by thermal formation of the DA adducts, leading to thermoreversible PCL networks exhibiting excellent shape-memory properties. Therefore, the same PCL_{76}-4OH has been selected and endfunctionalized by a coumarin derivative, i.e., a photodimerizable group to achieve PCL-based SMP materials by photocross-linking. The followed functionalization strategy is described in Scheme 2.

With the purpose to graft 4-methylcoumarin moieties at the PCL chain-ends, 7-hydroxypropoxy-4-methylcoumarin was synthesized by reaction between 7-hydroxy-4-methylcoumarin and 3-bromo-1-propanol, in the presence of potassium carbonate in DMF at 70 °C (Scheme 2). This first step was necessary to avoid the possible photo-Fries rearrangement of phenolic esters under ulterior UV irradiation.[35] The selection of 3-bromo-1-propanol was made instead of 2-bromoethanol, known to generate ethylene oxide side product under basic conditions. After two recrystallizations in toluene, a lightyellow solid was recovered. The ^{1}H NMR spectrum confirmed that the 7-hydroxypropyl-4-

Published in : Macromolecules (2019), vol.52x, n°52, pp. 444–456
DOI: 10.1021/acs.macromol.8b02188
Status : Postprint (Author's version)

methylcoumarin was successfully synthesized with a high purity (see Figure S1 in the Supporting Information).

Scheme 2. Strategy Applied for the Functionalization of 4-Arm Star-Shaped PCL by 4-Methylcoumarin Moieties

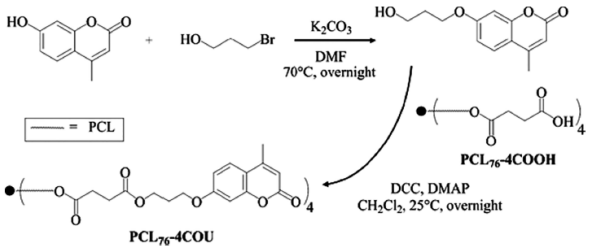

Four-arm star-shaped PCL end-capped by coumarin moieties (PCL_{76}-4COU) was synthesized via two consecutive esterification steps, as described previously.[13] In the first step, PCL_{76}-4OH was quantitatively converted to PCL_{76}-4COOH by the reaction of the hydroxyl end-groups with succinic anhydride. In the second step, PCL_{76}-4COOH was reacted with an excess of 7-hydroxypropoxy-4-methylcoumarin, in the presence of DCC and DMAP, according to a Steglich esterification procedure (Scheme 2). The conversion of the carboxylic acid chain-ends into 4-methylcoumarin was determined by ^{1}H NMR (Figure 1) by comparison of the integral of the signal of the CH_2–O–Ph (protons E, Figure 1) of coumarin and the integral of the signal of the (O)C–CH_2– CH_2–C(O) (protons I, Figure 1) of PCL_{76}-4COOH and was equal to 95%. This functionalization yield is similar to the ones reported for furan and maleimide functionalized PCL_{76}4COOH by the same reaction.

The SEC traces of PCL_{76}-4OH (red curve, Figure S2) and PCL_{76}-4COU (green curve, Figure S2) using a differential refractometer overlapped, despite the chain-ends modification, confirming that no side-reaction or degradation occurred. Moreover, the UV absorption SEC trace of PCL_{76}-4COU (purple curve, Figure S2) confirms the functionalization of PCL by 4-methylcoumarin moieties.

The macromolecular parameters of the PCL precursors are summarized in Table 1.

Photoinduced Cross-Linking and Swelling Experiments. Before UV irradiation, the PCL_{76}-4COU powder was compression-molded at 80 °C as well-defined disks (diameter= 25 mm, thickness = 0.5 mm) and then placed in a homemade mold for irradiation. To investigate the effect of the presence of a photosensitizer on the coumarin dimerization kinetics during UV irradiation, 25 mol % (PCL_{76}-4COUBzph$_{25}$) or 50 mol % of benzophenone (PCL_{76}-4COU-Bzph$_{50}$) (compared to coumarin) was added to the PCL_{76}-4COU. To get homogeneous dispersions of benzophenone in the bulk, PCL_{76}-4COU and benzophenone were dissolved in toluene, followed by the evaporation of the solvent, and then processed under the same conditions as the samples without benzophenone. In the following part of this paper, PCL_{76}4COU-Bzph$_0$ will refer to the sample without benzophenone. A homemade mold (disk of 2.5 cm in diameter and 0.5 mm of thickness) allowing light irradiation at 60 °C has been especially designed to prevent the formation of an irregular surface during UV irradiation and ensure reproducibility (Figure 2). The template containing the PCL sample was sandwiched between two films of cross-linked polydimethylsiloxane (PDMS), preventing the adhesion of cross-linked PCL to the quartz plates used to provide rigidity, which are both transparent to UV irradiation.

Published in : Macromolecules (2019), vol.52x, n°52, pp. 444–456
DOI: 10.1021/acs.macromol.8b02188
Status : Postprint (Author's version)

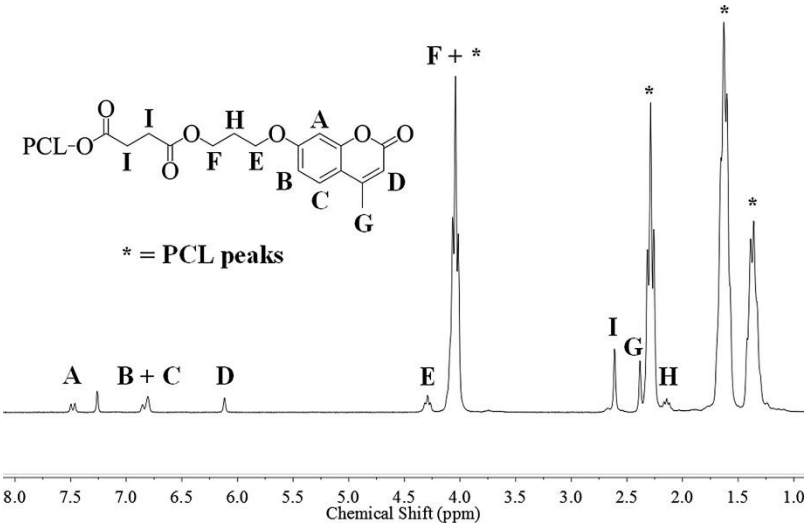

Figure 1. 1H NMR spectrum of PCL76-4COU.

Table 1. Macromolecular Parameters of the Chain-Ends Functional PCL

	chain-ends conv[a] (%)	$\bar{M}_n$ (^{1}H NMR)[b] (g/mol)	$Đ$ (SEC)[c]
PCL_{76}-4OH	n/a	8800	1.18
PCL_{76}-4COOH	100	9200	1.15
PCL_{76}-4COU	95	10100	1.20

[a]Conversion of the hydroxyl chain-end into carboxylic acid or coumarin determined by ^{1}H NMR. [b]Average molar mass (PCL_{76}-4OH: 76 × 114 g/mol + 136.14 g/mol; PCL_{76}-4COOH: M_n PCL_{76}-4OH + 400 g/mol; PCL_{76}-4COU: M_n PCL_{76}-4COOH + 937 g/mol × 0.95). [c]Molar mass distribution measured by SEC in THF at 45 °C.

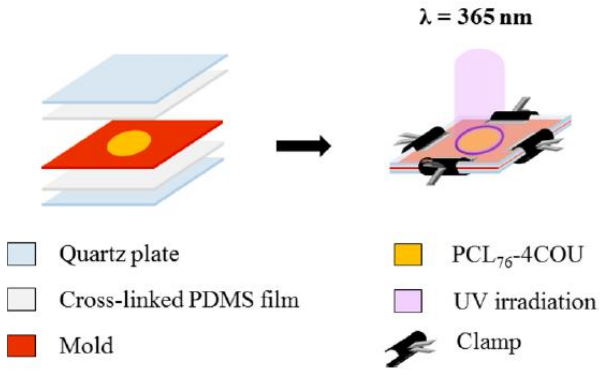

Figure 2. Design of the UV-curing mold.

Published in : Macromolecules (2019), vol.52x, n°52, pp. 444–456
DOI: 10.1021/acs.macromol.8b02188
Status : Postprint (Author's version)

The system was then fixed with four clamps to maintain together the different parts and placed under UV irradiation at 365 nm.

Because we are ultimately interested by shape-memory properties of the PCL networks, the selected star-shaped PCL is by purpose semicrystalline. Therefore, the UV-curing was performed at 60 °C, i.e., above the melting temperature of the PCL, to confer enough mobility to the PCL chains and thus transparency. The cross-linking kinetics of PCL_{76}-4COU was first followed by swelling experiments, performed in $CHCl_3$, a good solvent of the PCL, to determine the insoluble fraction and the swelling ratio of the sample in function of UV curing times and benzophenone content. Figure 3a reports these data for the system in the absence of benzophenone and shows the progressive network formation over an irradiation period of 6h.

After 60 min, the insoluble fraction is already above 50%. After 360 min of irradiation at 60 °C, a plateau is reached for both insoluble fraction and swelling ratio at 99.1% and 800%, respectively. These data clearly evidence the high rate and efficiency of the photo-cross-linking as compared to thermal DA adduct cross-linking for which the plateau is reached after 24 h, forming a less dense network characterized by a swelling ratio of 1500%.[14] To reach the same swelling ratio of 1500%, the PCL_{76}-4COU requires irradiation only for a period of <120 min.

In the presence of benzophenone (Figure 3b), the crosslinking rate was speeded up dramatically as demonstrated by an insoluble fraction >93% after 5 min of irradiation. Indeed, in the presence of benzophenone, the dimerization of coumarins takes place via a triplet state pathway in contrast to the reaction without photosensitizer, occurring via a singlet state pathway. As the triplet state has a longer lifetime (0.1–100 s) than the singlet state (10^{-9}–10^{-7} s), the number of effective collisions increases in the presence of benzophenone leading to faster kinetics.[19] The cross-linking profile is also found dependent on the benzophenone concentration. Indeed, the plateau is reached after 60 and 30 min for PCL_{76}-4COU-$Bzph_{25}$ and PCL_{76}-4COU-$Bzph_{50}$, respectively. Nevertheless, in both cases, an insoluble fraction of 100% and a swelling ratio of 550% were reached at the plateau, corresponding to a similar and highly cross-linking node density for both blends containing benzophenone. Remarkably, to reach the swelling ratio of 800% (obtained after 360 min without benzophenone), i.e., similar network cross-link density, irradiation times between 10 and 20 min are enough in the presence of benzophenone.

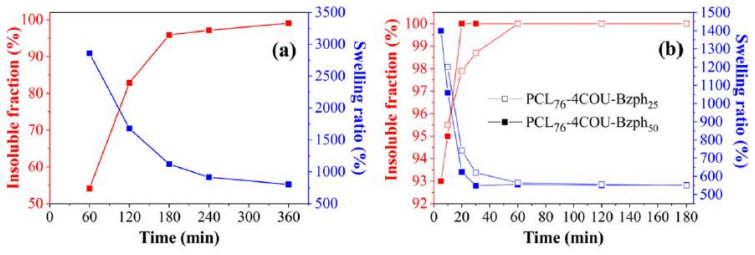

Figure 3. Evolution of the insoluble fraction and of the swelling ratio for (a) PCL_{76}-4COU-$Bzph_0$ and (b) PCL_{76}-4COU-$Bzph_{25}$ (open symbols) and PCL_{76}-4COU-$Bzph_{50}$ (closed symbols) measured in $CHCl_3$ as a function of UV curing time at 60 °C.

Published in : Macromolecules (2019), vol.52x, n°52, pp. 444–456
DOI: 10.1021/acs.macromol.8b02188
Status : Postprint (Author's version)

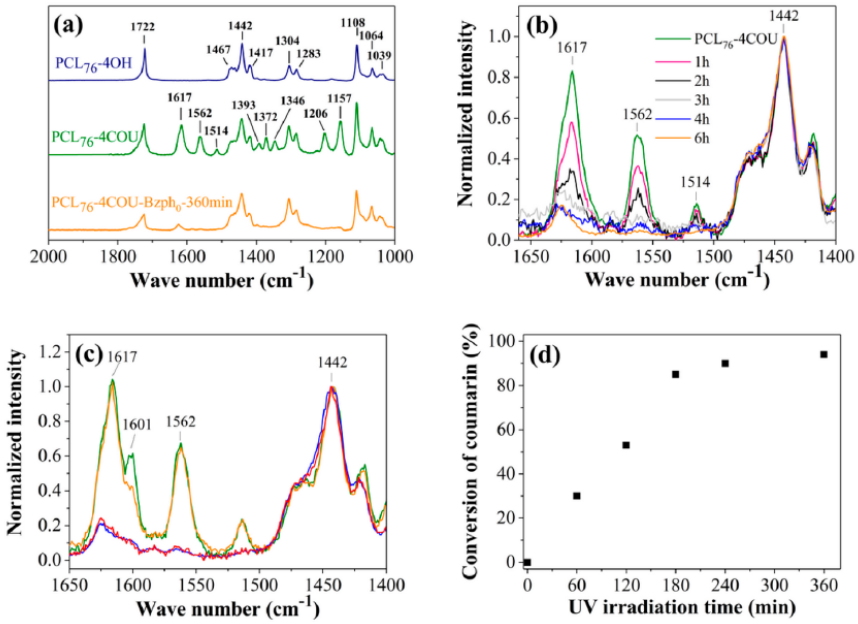

Figure 4. (a) Full Raman spectra of PCL_{76}-4OH (navy blue curve), PCL_{76}-4COU (green curve), and PCL_{76}-4COU-$Bzph_0$ after 360 min of UV irradiation (orange curve). (b) Raman spectra between 1650 and 1400 cm^{-1} of PCL_{76}-4COU-$Bzph_0$ before UV irradiation (green curve), after 60 min (pink curve), after 120 min (black curve), after 180 min (gray curve), after 240 min (navy blue curve), and after 360 min of UV irradiation (orange curve). (c) Raman spectra between 1650 and 1400 cm^{-1} of PCL-4COU-$Bzph_{25}$ (orange curve) and PCL-4COU-$Bzph_{50}$ (green curve) before UV irradiation and PCL-4COU-$Bzph_{25}$ (red curve) and PCL-4COU-$Bzph_{50}$ (blue curve) after irradiation for 60 and 30 min, respectively. (d) Conversion of coumarin (%) as a function of UV irradiation time at 60 °C for PCL-4COU-$Bzph_0$.

Raman Study of the Network Formation. To quantify the coumarin dimerization yield in parallel to swelling experiments, Raman spectroscopy was performed to follow the intensity of the characteristic C═C stretching modes of coumarin groups.[22] Indeed, Raman spectroscopy is an efficient tool to quantify reaction yield since Raman intensities of the chain-end groups are proportional to their relative concentration in the material. This technique was already successfully applied in a previous work for the determination of DA reactions yield between furan and maleimide in a PCL-based network[14] for which it was found that the DA adduct formation yield leveled at 58% for the PCL network reaching a swelling ratio of 1500%.

Figure 4 compares the starting 4-arm star-shaped PCL before and after functionalization with coumarin. The apparition of the characteristic bands of coumarin in the 1100−1650 cm^{-1} window besides the ones of the PCL confirms the successful functionalization of the stars. The disappearance of these peaks after UV irradiation for 6 h without benzophenone confirms the coumarin conversion into the dimers.

Figure 4b compares the Raman spectra recorded after increasing UV irradiation times for the PCL_{76}-4COU-$Bzph_0$ and clearly evidence the progressive decrease of the coumarin band intensity in parallel to the irradiation time. From these spectra, the coumarin conversion is quantified versus time (Figure 4d). Similarly to the swelling ratio, the coumarin is rapidly consumed over the first 180 min and reaches a plateau after 360 min of irradiation at 365 nm. The conversion is then ∼94%. As expected by the lower swelling ratio (800%) reached at the plateau as compared to the DA adduct, a higher conversion of the coumarin dimers is reached than for the DA adduct (58% and 1500% of swelling ratio) at the plateau.[14] This is not surprising since the coumarin dimerization involves two identical molecules while

Published in : Macromolecules (2019), vol.52x, n°52, pp. 444–456
DOI: 10.1021/acs.macromol.8b02188
Status : Postprint (Author's version)

the formation of the DA adduct requires the reaction of two complementary groups: the diene (furan) and the dienophile (maleimide).

Interestingly, to obtain a network with a swelling ratio of 1500% with the coumarin system, one should irradiate a little bit less than 120 min, which would correspond to the conversion of about 55% of the coumarin based in Figure 4d data. This conversion is very close to the DA adduct formation yield leveled at 58% for the PCL network, reaching a swelling ratio of 1500%.[(14)]

In the presence of benzophenone, the Raman spectra before irradiation are almost superimposed (Figure 4c) whatever the content in benzophenone except for a new Raman band appearing at 1601 cm^{-1}, which corresponds to the stretching mode of the C═C of the benzophenone.

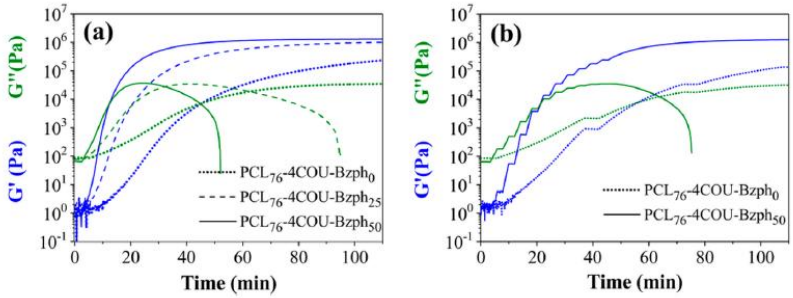

Figure 5. (a) Evolution of the storage modulus (G') in blue and loss modulus (G'') in green for PCL_{76}-4COU-$Bzph_0$ (dotted curves), PCL_{76}-4COU-$Bzph_{25}$ (dashed curves), and PCL_{76}-4COU-$Bzph_{50}$ (solid curves) under UV irradiation at 365 nm. (b) Switching on/off cycles for PCL_{76}-4COU-$Bzph_0$ (dotted curves) and PCL_{76}-4COU-$Bzph_{50}$ (solid curves).

After 30 min (for PCL_{76}-4COU-$Bzph_{50}$) or 60 min (for PCL_{76}-4COU-$Bzph_{25}$) of UV irradiation, the intensity of the band at 1562 cm^{-1} decreases sharply to almost zero in both samples, corresponding to a quantitative dimerization of coumarin. These results show that the conversion of coumarin in its dimer is total for both blends containing benzophenone in contrast to PCL_{76}4COU-$Bzph_0$ for which 6% of coumarin remains unreacted. Therefore, a higher cross-linking density is expected for the blends, which is in line with the swelling experiments. It is worth mentioning that both sides of the samples were analyzed by Raman spectroscopy. The same conversion of the coumarin into the corresponding dimer was observed, which evidences the good penetration of the UV light throughout the entire sample (thickness typically 0.5 mm), leading to a homogeneous cross-linking density in the whole thickness.

Rheological Study of the Network Formation Kinetics. The formation of the network induced by the dimerization of the coumarins was then investigated by rheology experiments under UV irradiation at 365 nm at 60 °C, using a reflecting mirror to focus the UV light source on the sample (see Figure S3 in the Supporting Information).

As pointed out by Winter et al., the determination of the point (temperature or time), where the tan δ is independent of the frequency, is generally accepted as the most accurate method to bring out the gel point.[(36)] However, the elastic modulus (G')–loss modulus (G'') crossover is much more easily determined and can be considered as the gel point for systems that exhibit, when reaching the gel point, a power law behavior $\mathbf{G}'(\omega) = G''(\omega) \sim \omega^n$ with a specific exponent value n = 1/2. This is particularly the case for stoichiometric balanced systems far above glass and melting transition temperature, which is the case of the systems studied at 60 °C. In Figure 5b, the storage modulus (G') and the loss modulus

Published in : Macromolecules (2019), vol.52x, n°52, pp. 444–456
DOI: 10.1021/acs.macromol.8b02188
Status : Postprint (Author's version)

(G") are measured as a function of time to follow the formation of the network by the dimerization of coumarins.

In the beginning of the analysis at 60°, before switching on the UV light at 365 nm, the loss modulus (G") is higher than the elastic modulus (G') for all the blends, which was expected for a polymer above its melting temperature. After 2 min at 60 °C, the UV light is switched on and both moduli directly increased in the function of time. The increase is faster for G' than for G", and the gel point is reached after 9, 18, and 40 min for PCL_{76}-4COU-$Bzph_{50}$, PCL_{76}-4COU-$Bzph_{25}$, and PCL_{76}4COU-$Bzph_0$, respectively (Table 2).

As previously demonstrated by the swelling experiments, these results confirmed that benzophenone fasten the formation of the chemical network since lower gelation time is observed for increasing content of benzophenone.

Table 2. Rheological Data Extracted from Figure 5a for Cross-Linking at 60 °C under UV Irradiation

blends	$G'_{gel\ point}$ [a] (Pa)	$t_{gel\ point}$ [b] (min)	G'_{end} [c] (Pa)	G''_{end} [d] (Pa)
PCL_{76}-4COU-$Bzph_0$	7300	40	2.34×10^5	34400
PCL_{76}-4COU-$Bzph_{25}$	7100	18	9.78×10^5	<0
PCL_{76}-4COU-$Bzph_{50}$	7200	9	1.32×10^6	<0

[a]Elastic modulus (Pa) at the gel point at 60 °C under UV irradiation. [b]Time (min) required to reach the gel point at 60 °C under UV irradiation. [c]Elastic modulus (Pa) after 110 min at 60 °C under UV irradiation. [d]Loss modulus (Pa) after 110 min at 60 °C under UV irradiation.

In addition, the values of $G'_{gel\ point}$ for all three systems were very close, traducing a similar cross-linking density at the gel point. It should be pointed out that the G" values tend to zero after 50 and 95 min of irradiation for PCL_{76}-4COU-$Bzph_{50}$ and PCL_{76}-4COU-$Bzph_{25}$, confirming the formation of highly cross-linked materials with an almost perfect elastic behavior in the presence of benzophenone, which is in line with high conversion of the coumarin into dimers (close to 100%) as demonstrated by Raman spectroscopy and very low swelling ratio (550%).

To demonstrate that UV-induced dimerization of coumarins allows a thorough control of the formation of the network by switching on/off the UV lamp, similar rheological measurements were performed at 60 °C with UV switching on/off cycles on PCL_{76}-4COU-$Bzph_0$ (UV light switched-on: 30 min/ switched-off: 5 min) and PCL_{76}-4COU-$Bzph_{50}$ (UV light switched-on: 2 min/switched-off: 2 min) (Figure 5b).

Under UV irradiation, both G' and G" moduli increased as a function of time due to the formation of the network by dimerization of coumarins. When the UV lamp is switched off, the increase of both moduli directly stopped, and G' and G" remain constant as a function of time since coumarin dimerization does not occur. By switching the UV irradiation back on, both moduli directly increased again. Interestingly, by removing the switching-off segments of the curves presented in Figure 5b, the curves are perfectly superimposed with those presented in Figure 5a (Figure 6a,b).

Published in : Macromolecules (2019), vol.52x, n°52, pp. 444–456
DOI: 10.1021/acs.macromol.8b02188
Status : Postprint (Author's version)

Remarkably, this experiment shows that the cross-linking degree of the network can be precisely controlled by the irradiation time. Frequency sweep experiments performed after110 min of UV curing at 60 °C confirm that no relaxation occurs during the rheological experiments (see Figure S4).

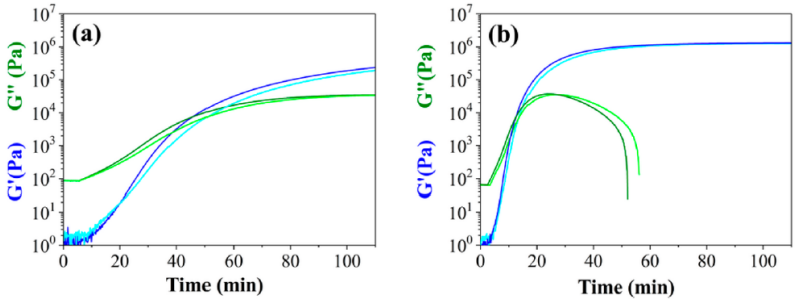

Figure 6. Overlay of switching on−off time sweep experiment (G' in light blue and G'' in light green) with classical time sweep experiment (G' in blue and G'' in green) at 60 °C under irradiation at 365 nm for (a) PCL_{76}-4COU-$Bzph_0$ and (b) PCL_{76}-4COU-$Bzph_{50}$.

Crystallinity Degrees of PCL-Based Networks. Prior to shape-memory characterizations, the degree of crystallinity (X_c), the melting temperature (T_m), and the crystallization temperature (T_c) of the three types of cross-linked PCL materials were determined by DSC, these characteristics being important for the fixity properties of the shape-memory materials, and compared to non-cross-linked and DA crosslinked systems (Table 3).

$$X_c = \frac{\Delta H_f(T_m)}{\Delta H_f^0(T_m^0)} \times 100 \qquad (4)$$

Table 3. Thermal Properties Extracted from DSC Thermograms and Swelling Ratio

	irradiation time (min)	X_c [a]	T_c (°C)	T_m (°C)	SR (%)
PCL_{76}-4COU	0	59	28	50	n/a
PCL_{76}-4COU-$Bzph_0$-120min	120	28	10	40	1300
PCL_{76}-4COU-$Bzph_0$-360min	360	35	7	38	800
PCL_{76}-4COU-$Bzph_{25}$-60min	60	25	−14	34	550
PCL_{76}-4COU-$Bzph_{50}$-5min	5	29	20	44	1400
PCL_{76}-4COU-$Bzph_{50}$-30min	30	18	−19/−16	31	550
PCL_{76}-4FUR/PCL_{76}-4MAL	n.a.	37	22	44	1500

[a]The degree of crystallinity was calculated according to eq 4 in which $\Delta H_f(T_m)$ is the enthalpy of melting measured by DSC and $\Delta H_f^0(T_m^0)$ is the enthalpy of melting for a 100% crystalline PCL, equal to 139.5 J g^{-1} according to the literature [Crescenzi, V.; Manzini, G.; Calzolari, G.; Borri, C. *Eur. Polym. J.* **1972**, *8*, 449].

As expected, increasing the cross-linking density decreases the melting temperature.[22] PCL_{76}-4COU-$Bzph_0$-120min and PCL_{76}-4COU-$Bzph_0$-360min were characterized by T_m of 40 and 38 °C and a degree of crystallinity of 28 and 35%, respectively, which are slightly lower than the values determined for DA-based PCL-network reported previously ($T_m \approx 45$ °C and degree of crystallinity ≈ 37%)[13] due to the higher cross-linking density of the coumarin-based networks. The crystallization temperature is significantly lower (5−7 °C), which was attributed to a hindered crystallization, usually leading to crystallites of

Published in : Macromolecules (2019), vol.52x, n°52, pp. 444–456
DOI: 10.1021/acs.macromol.8b02188
Status : Postprint (Author's version)

smaller size. This effect is clearly enhanced in network containing benzophenone. Surprisingly, the T_m of PCL_{76}-4COU-$Bzph_0$-120min is lower than for PCL_{76}-4COU-$Bzph_0$-360min, which is more cross-linked than the former one. For networks containing benzophenone, a sharp decrease of the transition temperatures was observed for PCL_{76}-4COU-$Bzph_{25}$-60min and PCL_{76}-4COU-$Bzph_{50}$-30min, with a T_m of 34 and 31 °C and a T_c of −14 and −19 °C, respectively. These shifts of T_m and T_c toward lower values are explained by the formation of more dense networks.[22] In PCL_{76}-4COU-$Bzph_{25}$-60min and PCL_{76}-4COU-$Bzph_{50}$-30min samples, the lower mobility of the polymer chains partially hindered the crystallization of PCL (decreasing T_c), leading to the formation of less stable crystallites, characterized by lower T_m and lower degree of crystallinity, typically 25 and 18%, respectively. Moreover, for PCL_{76}-4COU-$Bzph_{50}$-30min, the crystallization endotherm during cooling the sample is really low comparing to other systems (Figure 7). Despite the application of a slow temperature ramp (3 °C/min), PCL chains could not fully crystallize and a second crystallization endotherm was observed during the second heating cycle at similar temperature.

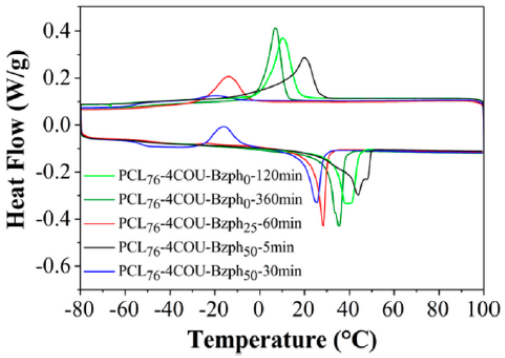

Figure 7. DSC thermograms of PCL_{76}-4COU-$Bzph_0$-120min (light green curve), PCL_{76}-4COU-$Bzph_0$-360min (green curve), PCL_{76}-4COU-$Bzph_{25}$-60min (red curve), PCL_{76}-4COU-$Bzph_{50}$-5min (black curve), and PCL_{76}-4COU-$Bzph_{50}$-30min (blue curve).

Because coumarin dimerization allows a thorough control of the formation of the network, a less crosslinked material, based on PCL_{76}-4COU-$Bzph_{50}$, was prepared by irradiation at 365 nm during a very short time (5 min instead of 30 min). Compared to PCL_{76}-4COU-$Bzph_{50}$-30min (swelling ratio of 550%), PCL_{76}-4COU-$Bzph_{50}$-5min (swelling ratio of 1400%) was characterized by a higher degree of crystallinity (29% instead of 18%), a higher T_m (44 °C instead of 31 °C), and a dramatically higher T_c (20 °C instead of −19 °C). This confirms that the cross-linking density of the network has a strong effect on the ability of the PCL chains to crystallize.

Published in : Macromolecules (2019), vol.52x, n°52, pp. 444–456
DOI: 10.1021/acs.macromol.8b02188
Status : Postprint (Author's version)

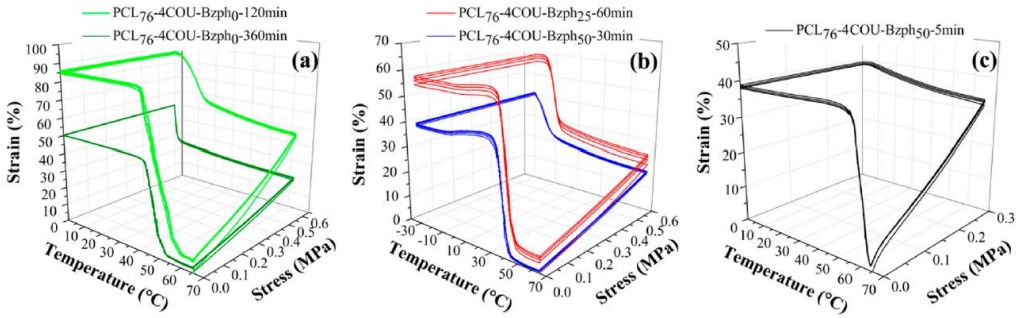

Figure 8. Shape-memory experiments (four cycles) of (a) PCL_{76}-4COU-$Bzph_0$-120min (light green curve) and PCL_{76}-4COU-$Bzph_0$-360min (green curve), (b) PCL_{76}-4COU-$Bzph_{25}$-60min (red curve) and PCL_{76}-4COU-$Bzph_{50}$-30min (blue curve), and (c) PCL_{76}-4COU-$Bzph_{50}$-5min (black curve).

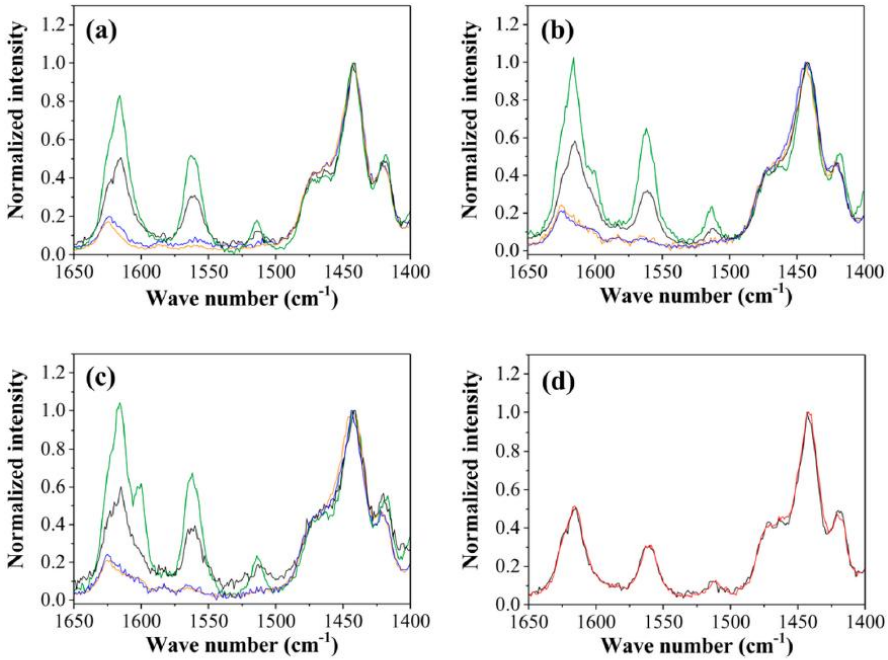

Figure 9. Raman spectra between 1650 and 1400 cm^{-1} before UV irradiation (green curve), after a first UV irradiation at 365 nm (orange curve), after UV irradiation at 365 nm and then at 256 nm for 60 min (black curve), and after UV irradiation at 365 nm and then at 256 and 365 nm (blue curve) for (a) PCL_{76}-4COU-$Bzph_0$, UV irradiation at 365 nm for 360 min; (b) PCL_{76}-4COU-$Bzph_{25}$, UV irradiation at 365 nm for 60 min; (c) PCL_{76}-4COU-$Bzph_{50}$, UV irradiation at 365 nm for 30 min; and (d) PCL_{76}-4COU-$Bzph_0$-360min after UV irradiation at 256 nm for 60 min (black curve) and 120 min (red curve).

Even if some samples are less crystalline, the three types of samples have been analyzed by DMA as shape-memory materials since cooling under stress usually favors the crystallization. Nevertheless, based on Table 3 data, the temperature to fix the temporary shape has to be adjusted to achieve enough crystallinity.

Shape-Memory Properties. The shape-memory properties of the materials were then studied by DMA by the application of four shape-memory cycles. The samples are heated at 65 °C and deformed by the application of a stress of 0.6 MPa, except for PCL_{76}-4COU-$Bzph_{50}$-5min sample, which brakes above 0.5 MPa and for which a stress of 0.3 MPa is applied. The samples are then cooled at a temperature lower than the crystallization temperature, i.e., 0 °C for PCL_{76}4COU-$Bzph_0$-120min, PCL_{76}-4COU-$Bzph_0$-360min, and PCL_{76}-4COU-$Bzph_{50}$-5min and −30 °C for PCL_{76}-4COUBzph$_{25}$-60min and PCL_{76}-4COU-$Bzph_{50}$-30min, to fix the temporary shape by PCL segments crystallization. The stress is then released and the samples are heated above the melting temperature, leading to their relaxation to the

Published in : Macromolecules (2019), vol.52x, n°52, pp. 444–456
DOI: 10.1021/acs.macromol.8b02188
Status : Postprint (Author's version)

permanent shape. Heating and cooling ramps applied to the sample are the same than in DSC experiment (3 °C/min) to correlate the results of DSC and DMA experiments. These shape-memory experiments are presented in Figure 8.

The shape fixity ratio, which is the ability of the sample to stay in its temporary shape after unloading, was calculated according to eq 5.

$$R_f\ (\%) = \frac{\varepsilon_u}{\varepsilon_m} \times 100 \qquad (5)$$

in which ε_m is the strain after stretching and cooling (maximums train) and ε_u is the strain after stress release. The recovery ratio (%) was calculated according to eq 6.

$$R_r\ (\%) = \left(\frac{\varepsilon_m - \varepsilon_p(N)}{\varepsilon_m - \varepsilon_p(N-1)} \right) \times 100 \qquad (6)$$

in which ε_m is the maximum strain and $\varepsilon_p(N-1)$ and $\varepsilon_p(N)$ are the strain in two successive cycles, before application of the stress. Fixity and recovery ratios are reported in Table S1 of the Supporting Information.

Expectedly, under the same applied stress, the maximum strain of PCL_{76}-4COU-$Bzph_0$-120min is higher than for PCL_{76}-4COU-$Bzph_0$-360min (Figure 8a) due to a lower cross-linking density (swelling ratio of 1300% vs 800%). In both cases, the fixity ratio is >99% for each cycle. These results confirm that crystallites enable the efficient and fast formation of switching domains, allowing the fixation of the temporary shape. The first cycle was characterized by an incomplete shape recovery ratio, i.e., strain at the start and end of a complete shape-memory cycle, of 93%, known as the training phenomenon,[37] while the following cycles were characterized by excellent shape recovery ratios, i.e., >98%. In contrast to DA-based SMP materials synthesized in previous works,[12] almost no creep effect was observed during the temporary shape formation, typically <1% for both PCL_{76}-4COU-$Bzph_0$ and PCL_{76}-4COU-$Bzph_{50}$ samples and ~1% for PCL_{76}-4COU$Bzph_{25}$-60min. This can be explained by the thermostability of the coumarin dimers, contrary to the DA adducts.[12] In the case of PCL-based SMP materials containing benzophenone which experienced a stress of 0.6 MPa, a slight increase of the strain was observed during the heating cycle before relaxation of the material to its permanent shape (Figure 8b). This phenomenon can be attributed to the crystallization of PCL chains during the heating ramp, in line with the DSC experiments. Nevertheless, both samples show high fixity ratio (>99%) and recovery (>98%). Interestingly, rheology has demonstrated the remote control of the cross-linking by the UV irradiation. By tuning the irradiation time, the cross-linking density can be easily adjusted and as a consequence the SMP of the material. This is illustrated in Figure 8c which shows the shape-memory cycle for the sample PCL_{76}-4COU-$Bzph_{50}$ after a shorter time of irradiation, i.e., 5 min rather than 30 min, to voluntary decrease the cross-linking density of the material. As evidenced by Figure 8c, the stress to be applied to reach 40% of deformation is divided by 2 (0.3 MPa) as compared to the sample irradiated for 30 min. (blue curve in Figure 8b). Remarkably, this sample still possesses a high shape fixity and recovery. Clearly, the modulus of the SMP can thus be easily tuned by controlling the irradiation time and so the SMP properties.

Published in : Macromolecules (2019), vol.52x, n°52, pp. 444–456
DOI: 10.1021/acs.macromol.8b02188
Status : Postprint (Author's version)

Photoreversibility of the Cross-Linking. The cleavage of the network by dissociation of the coumarin dimer was then investigated. Typically, the cross-linked materials were irradiated with a laser emitting UV light at 256 nm (UV intensity of ∼10 mW cm^{-2}) at 60 °C on a heating plate before being analyzed by Raman spectroscopy to quantify the regeneration of coumarin moieties (Figure 9).

The green curve of Figure 9a corresponds to the PCL_{76}4COU-$Bzph_0$ before UV irradiation whereas the orange curve corresponds to the PCL_{76}-4COU-$Bzph_0$ after UV irradiation at 365 nm for 360 min (PCL_{76}-4COU-$Bzph_0$-360min). The strong decrease of the characteristic bands of coumarin at 1562 and 1617 cm^{-1} is clearly observed due to dimerization. The black curve of Figure 9a corresponds to the PCL_{76}-4COU$Bzph_0$-360min sample after UV irradiation at 256 nm for 60 min with the purpose to cleave back the coumarin dimers into coumarin moieties. As evidenced by the spectra (orange versus

black curves), the increase of the intensity of the bands at 1562 and 1617 cm^{-1} proves the partial cleavage of ∼50% of the dimers, as quantified according to eq 3. Figure 9d shows that UV irradiation for an additional 60 min did not allow the regeneration of additional coumarin moieties, which indicates that an equilibrium between the photocleavage and the photodimerization reaction was reached, as reported by Chen et al.[20]

Swelling experiment also confirms the dissociation of the coumarin dimers as a swelling ratio of 1400% was measured after irradiation at 256 nm (800% before irradiation at 256 nm). A second UV irradiation at 365 nm for 360 min of this dedimerized sample allowed the complete conversion of the regenerated coumarin groups into the corresponding dimers. Similar results were observed for both samples containing benzophenone, with an equilibrium reached after 60 min of irradiation at 256 nm and corresponding also to the regeneration of ∼50% of the coumarin moieties. Contrary to the photodimerization reaction, benzophenone does not influence the photocleavage of the cyclobutane ring. Let us mention that the sample did not flow at 60 °C after irradiation at 256 nm and thus kept its shape and dimension, most probably because the partial cleavage of the coumarin dimers does not allow to cross the gel point of the network, preventing recycling of the material in contrast to the DA adducts. A second irradiation at 365 nm of the benzophenone containing samples allowed a complete conversion of regenerated coumarin within 60 and 30 min for PCL_{76}-4COU-$Bzph_{25}$ and PCL_{76}-4COU-$Bzph_{50}$, respectively (Figure 9b,c).

For technical reasons, it was not possible to follow the evolution of the storage and loss moduli during an irradiation at 256 nm by rheology. Nevertheless, rheological characterization was still used to confirm the partial regeneration of coumarin moieties after an irradiation at 256 nm. The samples were first irradiated at 365 nm to cross-link the materials and then irradiated at 256 nm for 60 min at 60 °C on a heating plate. The samples were then placed in the rheometer to measure the evolution of the modulus upon a second UV irradiation at 365 nm (Figure 10). Table 4 reports the storage and loss modulus of the sample after each irradiation step. It is worth noting that the values after the first irradiation at 365 nm, performed in this case in an oven, are slightly different than the one obtained upon an irradiation at 365 nm in the rheometer (Figure 5 and Table 2) probably as a result of a different distribution of the irradiation in the oven and in the rheometer.

The results show that the irradiation at 256 nm induces a decrease of the storage modulus, confirming the partial breaking of the network. However, the storage modulus remains higher than the loss modulus, meaning that the UV irradiation at 256 nm did not allow crossing back the gel point. These

Published in : Macromolecules (2019), vol.52x, n°52, pp. 444–456
DOI: 10.1021/acs.macromol.8b02188
Status : Postprint (Author's version)

results are in accordance with Raman results since a regeneration of 50% of coumarin is not sufficient to fall down below the limit of the gel point, i.e., 33% of cross-linking bonds according to the Flory−Stockmayer equation.

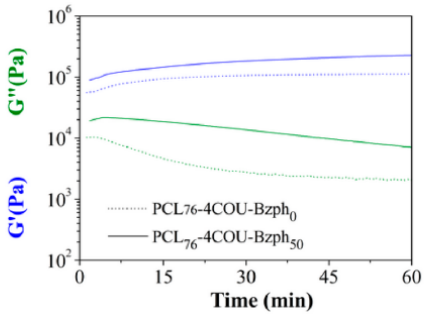

Figure 10. Evolution of the storage modulus (G') in blue and loss modulus (G'') in green for PCL_{76}-4COU-$Bzph_0$ (dotted curves) and PCL_{76}-4COU-$Bzph_{50}$ (solid curves) under UV irradiation at 365 nm and previously irradiated at 256 nm.

Table 4. Storage and Loss Moduli Extracted from Rheological Experiments on the Initial Network and after Each Irradiation Steps of Its "Recycling"

	1st irradiation at 365 nm		irradiation at 256 nm		2nd irradiation at 365 nm	
blends	G' (Pa)	G'' (Pa)	G' (Pa)	G'' (Pa)	G' (Pa)	G'' (Pa)
PCL_{76}-4COU-$Bzph_0$	114000	4200	55000	10300	112000	1900
PCL_{76}-4COU-$Bzph_{50}$	210000	5700	89000	19000	230000	6700

A second irradiation at 365 nm (Figure 10) induces a direct increase of the solid behavior of the samples traduced by the increase of the storage modulus and the decrease of the loss modulus; after irradiation at 365 nm, G' and G" values similar (within the experimental precision) to the ones measured for the initial network are reached (Table 4), showing that the network obtained after one cycle of irradiation (at 265 nm and then 365 nm) is similar to the initial one most probably due to the dimerization of all the regenerated coumarins, which is in line with the Raman data. In addition, SEC traces recorded on PCL stars before and after 1 h irradiation at 265 nm perfectly superimposed showing the stability of the coumarin-free polyester in these irradiation conditions. Therefore, it is not surprising to observe that the mechanical properties of the initial network are well preserved in the sample after one cycle of irradiation.

Being only partial, the reversible photocleavage of the network prevent the recycling of the material in contrast to DA adduct based network. Nevertheless, this partial reversibility can be advantageously used to reconfigure a new permanent shape to the material by the so-called solid-state plasticity as demonstrated qualitatively by the following experiment (see Figure S5). A sample of PCL_{76}-4COU-$Bzph_0$ irradiated at 365 nm for 360 min in the homemade mold, i.e., with a flat disk shape (permanent shape A), was placed at 60 °C under UV irradiation at 256 nm for 60 min to cleave some coumarin dimers. Then, still at 60 °C, the sample is bended and clamped on a support with an angle of 90° before being irradiated again at 365 nm for 360 min to dimerize the coumarin moieties of the material and fix a new bended permanent shape B. Let us mention that the UV curing time for the irradiation at 365 nm can

Published in : Macromolecules (2019), vol.52x, n°52, pp. 444–456
DOI: 10.1021/acs.macromol.8b02188
Status : Postprint (Author's version)

be reduced to 60 min for PCL_{76}-4COU-$Bzph_{25}$ and 30 min for PCL_{76}-4COU-$Bzph_{50}$ to reach the same permanent shape. This bended shape B is well a new permanent shape since the bending angle remains unchanged below and above the melting temperature. This confirms the ability to reconfigure the permanent shape of this material.

Both samples with the permanent shape A and B have then been involved in a shape-memory experiment. Deformation was then performed at 60 °C on both permanent shapes. By purpose, the temporary shapes were chosen to correspond to the same shapes A (flat disk) and B (bended disk) of the permanent samples. Therefore, the flat permanent shape A was bended at 90° to reach the shape B as temporary shape, and the permanent bended shape B was flattened by compression to reach the flat shape A as temporary shape. In both cases, excellent fixity and recovery were observed (Figure 11). This experiment shows that with this material an angle can be stored in a flat sample (permanent shape B) so as an angle can be erased by simple heating (permanent shape A), which offers strong potential for building more complex origami and selfdeploying constructs (see Figure S6 for an illustration of a more complex shape).

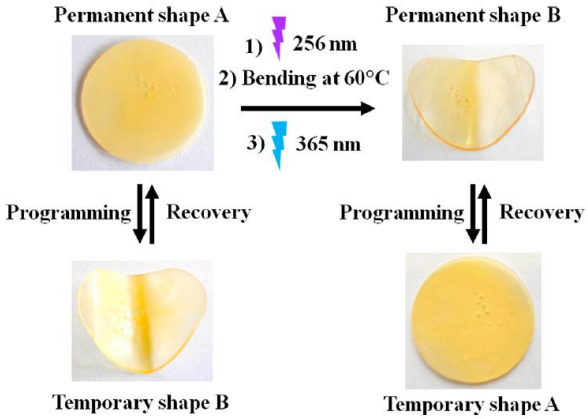

Figure 11. Qualitative demonstration of the shape-memory properties and of the reconfiguration of PCL_{76}-4COU-$Bzph_0$.

CONCLUSION

A 4-arm star-shaped PCL was successfully functionalized by 4methylcoumarin via an efficient two-step strategy and easily processed by compression molding before being cross-linked by UV irradiation at 365 nm by coumarin dimerization. According to swelling experiments, 360 min of UV irradiation is required to reach an almost quantitative conversion of coumarin. The formation of the network under UV irradiation at 365 nm was monitored online by rheology and confirms the efficient cross-linking of the PCL and the thorough control of the cross-linking process via an on/off switch of the UV light. The addition of benzophenone before UV curing dramatically increased the kinetics of the coumarin dimerization, with a full conversion after 60 or 30 min, as demonstrated by Raman spectroscopy analysis, for blends containing 25 or 50 mol % of benzophenone, respectively. The addition of benzophenone also leads to SMP materials with a higher cross-linking nodes density which are then characterized by lower T_c and T_m and lower degree of crystallinity compared to the SMP material without photosensitizer as pointed out by DSC experiments.

Published in : Macromolecules (2019), vol.52x, n°52, pp. 444–456
DOI: 10.1021/acs.macromol.8b02188
Status : Postprint (Author's version)

Consequently, the fixity temperature had to be decreased to lower temperature, i.e., −30 °C for the samples with benzophenone, which shows that a higher cross-linking of the samples is not necessarily better for shape-memory properties. This highlights the interest of this system, where the degree of cross-linking of the material can be easily controlled by simply switching off the UV irradiation at the appropriate time. For instance, a SMP material was already obtained after relatively short irradiation times typically 120 min in the absence of photosensitizer and 5 min in the presence of 50 mol % of benzophenone. In each case, the heat responsive SMP materials were characterized by excellent shape-memory fixity and recovery ratios. As demonstrated by Raman spectroscopy, the irradiation of the SMP materials at 256 nm allows the cleavage of half of coumarin dimers, which allows the reconfiguration of the permanent shape of the SMP by irradiation at 365 nm above 60 °C under stress. In contrast to DA-based SMP materials, characterized by a long curing time (typically 24 h) and creep occurring by retro-DA reaction under stress, coumarin dimerization presents some major advantages such as a short UV curing time (especially with 50 mol % of benzophenone) and excellent shape-memory properties without creep from cycle to cycle. Remarkably, the remote control of the network cross-linking density allows the fine-tuning of the shape-memory properties of these welldefined coumarin-based materials. The demonstrated photocontrolled solid-state plasticity allowing the reconfiguration of the permanent shape of the material combined with the excellent shape-memory properties of these networks able to form or erase angles easily, offering strong potential for building more complex origami and self-deploying constructs.

AUTHOR INFORMATION

Corresponding Author

*E-mail c.jerome@uliege.be.

ORCID

Christine Jerôme: 0000-0001-8442-5740

Notes

The authors declare no competing financial interest.

ACKNOWLEDGMENTS

The authors are grateful to Professor Bernard Gilbert for his valuable help in Raman spectroscopy. CERM thanks the Interuniversity Attraction Pole for granting the project "Functional Supramolecular Systems" (IAP7-5 FS2) and the DGO6 for supporting research in the frame of SMARTDIF project.

Published in : Macromolecules (2019), vol.52x, n°52, pp. 444–456
DOI: 10.1021/acs.macromol.8b02188
Status : Postprint (Author's version)

REFERENCES

(1) Lendlein, A.; Kelch, S. Shape-Memory Polymers. Angew. Chem., Int. Ed. 2002, 41 (12), 2034−2057.
(2) Lendlein, A.; Langer, R. Biodegradable, Elastic Shape-Memory Polymers for Potential Biomedical Applications. Science 2002, 296 (5573), 1673−1676.
(3) Liu, C.; Qin, H.; Mather, P. T. Review of progress in shapememory polymers. J. Mater. Chem. 2007, 17 (16), 1543−1558.
(4) Seward, K. P.; Krulevitch, P. A. Shape memory alloy/shape memory polymer tools. US20020142119A1, 2002.
(5) Maitland, D. J.; Metzger, M. F.; Schumann, D.; Lee, A.; Wilson, T. S. Photothermal properties of shape memory polymer microactuators for treating stroke*. Lasers Surg. Med. 2002, 30 (1), 1−11.
(6) Snyder, E. A.; Tong, T. H. Towards Novel Light-Activated Shape Memory Polymer: Thermomechanical Properties of Photoresponsive Polymers. MRS Online Proc. Libr. 2005, 872, J18.6.
(7) Jin Yoo, H.; Chae Jung, Y.; Gopal Sahoo, N.; Whan Cho, J. Polyurethane-Carbon Nanotube Nanocomposites Prepared by In-Situ Polymerization with Electroactive Shape Memory. J. Macromol. Sci., Part B: Phys. 2006, 45 (4), 441−451.
(8) Şener, S.; Sarıdoğan, E.; Staub, S.; Gök, M. O.; Bilir, M. Z.; Gürcüm, B. H. World Conference on Technology, Innovation and EntrepreneurshipShape-Memory Applications in Textile Design. Procedia - Social and Behavioral Sciences 2015, 195, 2160−2169.
(9) Sokolowski, W.; Metcalfe, A.; Hayashi, S.; Yahia, L.; Raymond, J. Medical applications of shape memory polymers. Biomed. Mater. 2007, 2 (1), S23.
(10) Lewis, C. L.; Dell, E. M. A review of shape memory polymers bearing reversible binding groups. J. Polym. Sci., Part B: Polym. Phys. 2016, 54, 1340.
(11) Habault, D.; Zhang, H.; Zhao, Y. Light-triggered self-healing and shape-memory polymers. Chem. Soc. Rev. 2013, 42 (17), 7244− 7256.
(12) Defize, T.; Riva, R.; Jerő me, C.; Alexandre, M. Multifunctional Poly(ϵ-caprolactone)-Forming Networks by Diels−Alder Cycloaddition: Effect of the Adduct on the Shape-Memory Properties. Macromol. Chem. Phys. 2012, 213 (2), 187−197.
(13) Defize, T.; Riva, R.; Raquez, J.-M.; Dubois, P.; Jerôme, C.; Alexandre, M. Thermoreversibly Crosslinked Poly(ε-caprolactone) as Recyclable Shape-Memory Polymer Network. Macromol. Rapid Commun. 2011, 32 (16), 1264−1269.
(14) Defize, T.; Thomassin, J.-M.; Alexandre, M.; Gilbert, B.; Riva, R.; Jerő me, C. Comprehensive study of the thermo-reversibility of Diels−Alder based PCL polymer networks. Polymer 2016, 84, 234− 242.
(15) Manouras, T.; Vamvakaki, M. Field responsive materials: photo-, electro-, magnetic- and ultrasound-sensitive polymers. Polym. Chem. 2017, 8 (1), 74−96.
(16) Jellali, R.; Bertrand, V.; Alexandre, M.; Rosiere, N.; Grauwels, M.; De Pauw-Gillet, M.-C.; Jerő me, C. Photoreversibility and Biocompatibility of Polydimethylsiloxane-Coumarin as Adjustable Intraocular Lens Material. Macromol. Biosci. 2017, 17, 1600495.
(17) Blasco, E.; Wegener, M.; Barner-Kowollik, C. Photochemically Driven Polymeric Network Formation: Synthesis and Applications. Adv. Mater. 2017, 29, 1604005.
(18) Chen, Y.; Chou, C. F. Reversible photodimerization of coumarin derivatives dispersed in poly(vinyl acetate). J. Polym. Sci., Part A: Polym. Chem. 1995, 33 (16), 2705−2714.
(19) Chen, Y.; Geh, J. L. Copolymers derived from 7-acryloyloxy-4methylcoumarin and acrylates: 1. Copolymerizability and photocrosslinking behaviours. Polymer 1996, 37 (20), 4473−4480.
(20) Chen, Y.; Wu, J. D. Preparation and photoreaction of copolymers derived from N-(1-phenylethyl)acrylamide and 7acryloyloxy-4-methyl coumarin. J. Polym. Sci., Part A: Polym. Chem. 1994, 32 (10), 1867−1875.
(21) Chen, Y.; Jean, C. S. Polyethers containing coumarin dimer components in the main chain. I. Synthesis by photopolymerization of 7,7′-(polymethylenedioxy) dicoumarins. J. Appl. Polym. Sci. 1997, 64 (9), 1749−1758.
(22) Seoane Rivero, R.; Bilbao Solaguren, P.; Gondra Zubieta, K.; Gonzalez-Jimenez, A.; Valentin, J. L.; Marcos-Fernandez, A. Synthesis and characterization of a photo-crosslinkable polyurethane based on a coumarin-containing polycaprolactone diol. Eur. Polym. J. 2016, 76, 245−255.
(23) Rivero, R. S.; Solaguren, P. B.; Zubieta, K. G.; Peponi, L.; Marcos-Fernandez, A. Synthesis, kinetics of photo-dimerization/ photo-cleavage and physical properties of coumarin-containing branched polyurethanes based on polycaprolactones. eXPRESS Polym. Lett. 2016, 10 (2), 84.
(24) Lendlein, A.; Jiang, H.; Junger, O.; Langer, R. Light-induced shape-memory polymers. Nature 2005, 434 (7035), 879−882.

Published in : Macromolecules (2019), vol.52x, n°52, pp. 444–456
DOI: 10.1021/acs.macromol.8b02188
Status : Postprint (Author's version)

(25) Rochette, J. M.; Ashby, V. S. Photoresponsive Polyesters for Tailorable Shape Memory Biomaterials. Macromolecules 2013, 46 (6), 2134−2140.
(26) Pilate, F.; Mincheva, R.; De Winter, J.; Gerbaux, P.; Wu, L.; Todd, R.; Raquez, J.-M.; Dubois, P. Design of MultistimuliResponsive Shape-Memory Polymer Materials by Reactive Extrusion. Chem. Mater. 2014, 26 (20), 5860−5867.
(27) Wu, L.; Jin, C.; Sun, X. Synthesis, Properties, and LightInduced Shape Memory Effect of Multiblock Polyesterurethanes Containing Biodegradable Segments and Pendant Cinnamamide Groups. Biomacromolecules 2011, 12 (1), 235−241.
(28) Xie, H.; Deng, X.-Y.; Cheng, C.-Y.; Yang, K.-K.; Wang, Y.-Z. New Strategy to Access Dual-Stimuli-Responsive Triple-ShapeMemory Effect in a Non-overlapping Pattern. Macromol. Rapid Commun. 2017, 38 (4), 1600664.
(29) Xie, H.; He, M.-j.; Deng, X.-Y.; Du, L.; Fan, C.-J.; Yang, K.-K.; Wang, Y.-Z. Design of Poly(l-lactide)−Poly(ethylene glycol) Copolymer with Light-Induced Shape-Memory Effect Triggered by Pendant Anthracene Groups. ACS Appl. Mater. Interfaces 2016, 8 (14), 9431− 9439.
(30) Jin, B.; Song, H.; Jiang, R.; Song, J.; Zhao, Q.; Xie, T. Programming a crystalline shape memory polymer network with thermo- and photo-reversible bonds toward a single-component soft robot. Science Advances 2018, 4 (1), eaao3865.
(31) Pilate, F.; Stoclet, G.; Mincheva, R.; Dubois, P.; Raquez, J.-M. Poly(ε-caprolactone) and Poly(ω-pentadecalactone)-Based Networks with Two-Way Shape-Memory Effect through [2 + 2] Cycloaddition Reactions. Macromol. Chem. Phys. 2018, 219 (4), 1700345.
(32) Nagata, M.; Yamamoto, Y. Photocurable Shape-Memory Copolymers of ε-Caprolactone and L-Lactide. Macromol. Chem. Phys. 2010, 211 (16), 1826−1835.
(33) Nagata, M.; Yamamoto, Y. Synthesis and characterization of photocrosslinked poly(ε-caprolactone)s showing shape-memory properties. J. Polym. Sci., Part A: Polym. Chem. 2009, 47 (9), 2422− 2433.
(34) Krier, F.; Riva, R.; Defrerè, S.; Mestdagt, M.; Van Langendonckt, A.; Drion, P.; Dehoux, J. P.; Donnez, J.; Foidart, J. M.; Jerome, C.; Evrard, B. Device-based controlled local delivery of́ anastrozol into peritoneal cavity: in vitro and in vivo evaluation. J. Drug Delivery Sci. Technol. 2014, 24 (2), 198−204.
(35) Bansal, R. K. Synthetic Approaches in Organic Chemistry, 1996.
(36) Winter, H. H. Can the gel point of a cross-linking polymer be detected by the G′ − G″ crossover? Polym. Eng. Sci. 1987, 27 (22), 1698−1702.
(37) Rousseau, I. A. Challenges of shape memory polymers: A review of the progress toward overcoming SMP's limitations. Polym. Eng. Sci. 2008, 48 (11), 2075−2089.